JOURNAL OF WATER AND LAND DEVELOPMENT
e-ISSN 2083-4535

Polish Academy of Sciences (PAN) Institute of Technology and Life Sciences – National Research Institute (ITP – PIB)

JOURNAL OF WATER AND LAND DEVELOPMENT
DOI: 10.24425/jwld.2026.157839
2026, No. 68 (I–III): 236–245

Soil erosion assessment using the erosion potential method – Case of Boussekour watershed, Central Rif, Morocco

Abdelhamid Tawfik, Issam Etebaai*, Mustapha Ait Omar, Soukaina Ed-Dakiri, Morad Taher

Abdelmalek Essaadi University, Faculty of Science and Technique, Al-Hoceima, Team of Applied Geosciences and Geological Engineering, Quartier M'haneche II, avenue 9 Avril, B.P. 2117, Tetouan, Morocco

* Corresponding author

RECEIVED 12.08.2025 ACCEPTED 27.11.2025 AVAILABLE ONLINE 31.03.2026

HIGHLIGHTS

- Quantitative soil loss assessment in a fragile Mediterranean watershed, Morocco.
- EPM and GIS mapping of soil water erosion vulnerability in Mediterranean watersheds.
- 45% of Boussekour watershed shows high soil loss (20–40 $Mg \cdot ha^{-1} \cdot yr^{-1}$).

Abstract: The human impact, combined with the geomorphological, lithological, and climatic specificities of northern Morocco, makes the soils highly vulnerable to the risk of water erosion. The primary purpose of this research is to map and assess the soil water erosion vulnerability in the Boussekour watershed, located in the Rif Mountain chain in northern Morocco, by applying the erosion potential method (EPM) developed by Gavrilović. It is an approach that involves integrating, within a Geographic Information System (GIS) environment, six parameters involved in the erosive phenomenon: temperature, rainfall, slope, soil erodibility, current erosion, and soil protection. The input data necessary for applying this model were derived from satellite images, digital elevation models (DEMs), granulometric and physico-chemical analyses of soil samples, and local rainfall data. Results show that the high erosion class (from 20 to 40 $Mg \cdot ha^{-1} \cdot yr^{-1}$) is prevalent and acts on 45% of the watershed, while the low (from 5 to 10 $Mg \cdot ha^{-1} \cdot yr^{-1}$) and very low (from 0 to 5 $Mg \cdot ha^{-1} \cdot yr^{-1}$) erosion classes account for just 6.98% and 1.44% of the area, respectively. This result demonstrates that the Boussekour watershed is profoundly threatened by soil water erosion, and an effort ought to be made to promote operative soil conservation efforts.

Keywords: erosion potential method (EPM), Geographic Information System (GIS), Morocco, soil water erosion, watershed

INTRODUCTION

Soil water erosion ranks among the major processes of land deterioration in Mediterranean countries, resulting from the complex natural conditions associated with the heavy human impact that has influenced and continues to influence them (Bou Kheir, Girard and Khawlie, 2001). Indeed, the Mediterranean region is characterised by a high percentage of sloping land, with around 45% of the region's land mass featuring slopes greater than8% (Franchis de, 2003), the frequent occurrence of intense rainfall (Defour, 2015), and the degradation of natural vegetation cover (Shakesby, 2011). These fragilities are exacerbated by growing demographic pressure, alarming climatic and socio-economic projections, which exert supplementary pressure on water and soil resources (Voltz *et al.*, 2018). The interplay of these factors results in excessive soil loss, which frequently exceeds the

intrinsic regenerative ability of the soil in several Mediterranean regions (Kosmas *et al*., 1997).

Morocco is no exception to the Mediterranean trend, with water erosion affecting approximately 40% of the country's land surface (Hudson, 1990) and threatening nearly 75% of its total catchment areas (HCEFLCD, 1996). Annual soil losses are estimated at around 100 Tg (Ministère de la Transition Energétique et du Développement Durable, 2020), with erosion rates ranging from 5 $Mg{\cdot}ha^{-1}{\cdot}yr^{-1}$ in the Middle Atlas to as much as 50 $Mg{\cdot}ha^{-1}{\cdot}yr^{-1}$ in the northern Rif (HCEFLCD, 2013).

The objective of the current study is to map model susceptibility to soil water erosion in the Boussekour catchment, located on north-facing slopes of the Central Rif Mountains in northern Morocco. This watershed is part of the Al Hoceima National Park, a protected area of high ecological value which has been listed since 2009 as a Specially Protected Area of Mediterranean Importance (SPAMI). This study is the first to assess water erosion in the Boussekour watershed. Recent studies in neighbouring catchments have recorded high erosion rates (Taher *et al*., 2022; Ed-Dakiri *et al*., 2024), which pose a threat to the local population, for whom agriculture is a crucial source of income. These conditions compel the local populations to emigrate to cities or overseas. The finding necessitates the adoption of efficient soil management and conservation policies, based on reliable assessments and spatialisation of water erosion risk (Borrelli *et al*., 2017).

Thanks to developments in remote sensing (RS) and geographic information systems (GIS), which are now accessible and low-cost (Bou Kheir, Girard and Khawlie, 2001; Akalai *et al*., 2014; Bachaoui *et al*., 2014), various methods are available to map model susceptibility to soil water erosion, such as universal soil loss equation (USLE), revised USLE (RUSLE), modified USLE (MUSLE), erosion potential method (EPM), soil and water assessment tool (SWAT), among others. The Gavrilović EPM method, based on mapping and combining erosion parameters within a GIS environment (Zahnoun *et al*., 2019), is among these established approaches. We selected it for this research due to its effectiveness and rapid implementation (Dragičević, Karleuša and Ožanić, 2016; Zeghmar, Marouf and Mokhtari, 2022; Milevski *et al*., 2024). Indeed, this is an approach which has proven successful in many countries worldwide, starting with Serbia (country of origin), Bosnia and Herzegovina, Chile, Greece, Iran, Iraq, Italy, Montenegro, the Republic of North Macedonia, and Slovenia, as well as North African countries such as Algeria, Morocco, and, to a lesser extent, Tunisia, where it delivered very satisfactory results.

MATERIALS AND METHODS

STUDY AREA

The Boussekour catchment is located on north-facing slopes of the Central Rif Mountains in northern Morocco, between latitudes 35° 14' and 35°00' N and longitudes 4°01' and 4°10' W (Fig. 1). With a Gravelius compactness index of approximately 1.69, it extends over an area of 208 km^2 in an elongated shape oriented southwest to northeast. Altitudes range from 1,193 m at the highest point to 0 m at the outlet, while slopes vary between 0° and 56°, with an average of 12.46°. The hydrographic network consists mainly of the

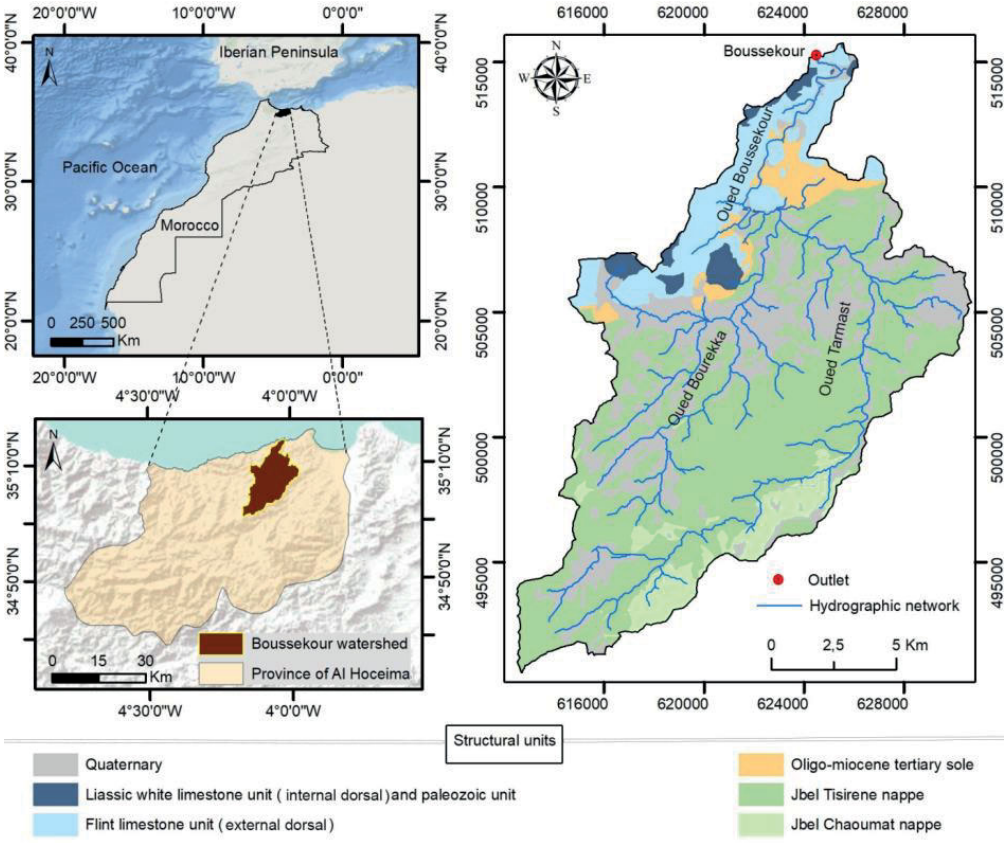

Fig. 1. Location and geological structural units of the Boussekour watershed; source: own elaboration

Boussekour wadi and its two main tributaries, the Bourekka wadi to the East and the Tarmast to the West.

The Boussekour watershed encompasses geological formations belonging to two structural domains of the Moroccan Rif Mountain range, namely the internal domain and the ultrarifian nappes. Thus, in the north-west, outcrops of the Bokkoya Massif appear, which is a mountain block belonging to the internal domain, composed of the flint limestone unit overlain by nappes in the form of klippes linked to the Liassic white limestone and Palaeozoic units. This massif lies above the marly series of the Tertiary sole, which in turn overlie the flysch formations of the ultrarifian nappes that cover the remainder of the basin.

The climate prevailing in the Boussekour watershed is a semi-arid climate featuring warm winters, characterised by rainfall exhibiting spatio-temporal irregularities, ranging from 200 mm·yr^{-1} during dry years and 330 mm·yr^{-1} in the wettest years.

The vegetation cover in the Boussekour watershed is markedly reduced. However, residual plant formations, located primarily in its northern part as low discontinuous matorral, remain interesting. They are dominated by species characteristic of the semi-arid Mediterranean stage, such as barbary thuya (*Tetraclinis articulata*), mastic tree (*Pistacia lentiscus*), French lavender (*Lavandula dentate*), and esparto grass (*Stipa tenacissima*). In this context, the production system relies on two closely interwoven and strictly complementary production subsystems: on the one hand, the cultivation of small cereal plots associated with fruit trees (almond (*Prunus dulcis*), fig (*Ficus carica*), and carob (*Ceratonia siliqua*)), sometimes intercropped with legumes (fava beans and peas); on the other hand, grazing on lands qualified as uncultivated, managed by the forestry service but claimed by farmers.

MATERIALS AND METHODS

The erosion potential method (EPM) method of Gavrilović, developed in the 1950s for the watersheds of former Yugoslavia, is an empirical model that enables the estimation of annual soil losses resulting from different types of erosion. This model is shown in Figure 2.

It integrates six key parameters (slope, soil erodibility, current erosion, soil protection, temperature, and precipitation) in a GIS environment using ArcGIS Pro software to calculate annual soil losses per Equation (1).

$$W = T \cdot H \cdot \pi \cdot \sqrt{Z^3} \tag{1}$$

where: W = average annual volume of soil loss (m^3·km^{-2}·yr^{-1}), T = temperature coefficient (–), H = annual precipitation (mm·yr^{-1}), π = mathematical constant equal to 3.14159 (–); Z = erosion intensity coefficient (–).

The temperature coefficient (T) is determined by Equation (2).

$$T = \sqrt{\frac{t_0}{10} + 0.1} \tag{2}$$

where: t_0 = average annual temperature (°C).

The erosion intensity coefficient (Z) is calculated using Equation (3).

$$Z = X_a \cdot Y \cdot \left(\varphi + \sqrt{J_a}\right) \tag{3}$$

where: X_a = soil protection coefficient (–), $0.01 \leq X_a \leq 1$, Y = soil erodibility coefficient (–), $0.1 \leq Y \leq 1$, φ = current erosion coefficient (–), $0.1 \leq \varphi \leq 1$, J_a = slope coefficient (%).

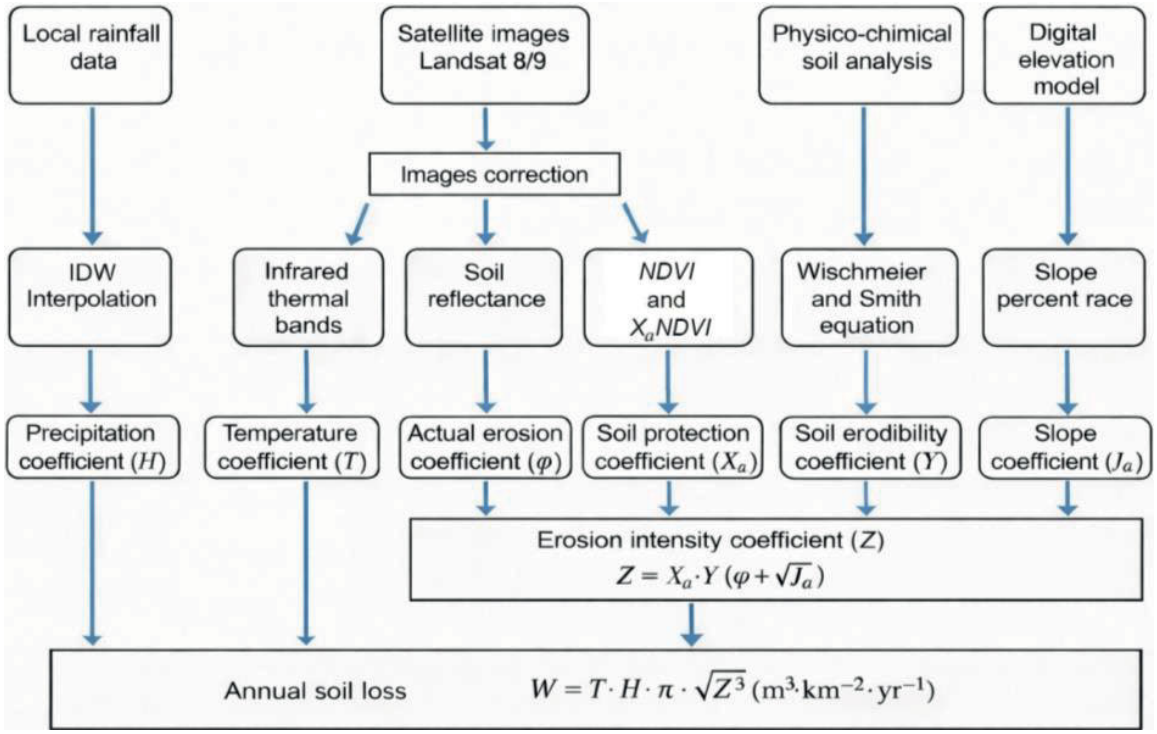

Fig. 2. Organisational chart of erosion potential method (EPM) used; *IDW* = inverse distance weighting, *NDVI* = normalised difference vegetation index, W = average annual volume of soil loss, π = mathematical constant, Z = erosion intensity coefficient; source: own elaboration

Temperature coefficient (*T*) – a key component of the EPM model developed by Gavrilović, highlights the crucial role of heat in intensifying erosive processes, particularly through increased soil water evaporation, desiccation, and crack formation (Lal, 2001). To map this parameter, a collection of Landsat 8/9 satellite images spanning different seasons of the 2022–2023 observation period was utilised, providing a detailed and localised representation of surface thermal conditions. This satellite-based approach has proven more reliable than interpolation methods based on meteorological station data, which often lack sufficient spatial resolution (Lakhili *et al.*, 2021).

The mapping of this parameter required the prior calculation of the average annual temperatures (t_0) at the watershed scale (Eq. 2). This step was performed by exploiting the thermal bands B10 and B11 of a time series of Landsat 8/9 images (2022–2023), representative of seasonal variations. The land surface temperature (*LST*) was derived for each band via Equation (4). The final value of t_0 is then obtained by averaging the *LSTs* of the spectral bands B10 and B11.

$$LST = \frac{BT}{1 + \left(\frac{\lambda \cdot BT}{\rho}\right)\ln(\varepsilon)} \tag{4}$$

where: BT = brightness temperature (°C), λ = effective wavelength of the thermal band (μm), ρ = $1.438 \cdot 10^{-2}$ m·K (Planck's second constant), ε = land surface emissivity (–).

The results indicate that temperature coefficient values exceed 1 across the entire Boussekour watershed (Fig. 3a), reflecting particularly high thermal conditions that increase the susceptibility of soils to water erosion.

Precipitation coefficient (*H*). Rainfalls among the key climatic factors influencing the processes of soil water erosion. From the very first drops, it initiates the detachment of soil particles; a process that continues through surface runoff and into the drainage network (Wischmeier and Smith, 1978; Morgan, 2009). Within the framework of this EPM method developed by Gavrilović (1988), rainfall is directly incorporated as annual averages expressed in millimetres, without transformation, due to its direct influence on sediment mobilisation potential. The precipitation coefficient map (Fig. 3b) was produced using Inverse Distance Weighting (IDW) interpolationin ArcGIS Pro, based on mean precipitation data recorded since 1982 from 8 rainfall stations: one positioned at the western boundary of the study area, with the remaining stations in proximity. The distribution of average rainfall across the Boussekour watershed reveals a slight increase in rainfall gradient, following a northeast-to-southwest axis.

Soil protection coefficient (X_a). The estimation of the soil protection coefficient (X_a) in the Boussekour watershed, based on the EPM method, relies on the average values of Normalised difference vegetation index (*NDVI*) derived from the same Landsat 8/9 satellite imagery used to determine the temperature coefficient. These *NDVI* values were corrected in accordance with the methodological criteria proposed by Zorn and Komac (2009), by capping the positive values at 0.6 for densely vegetated areas and the negative values at –0.19 for severely degraded environments such as badlands. This correction allowed for the generation of a modified *NDVI*, referred to as X_a *NDVI*, which was then used to calculate the X_a coefficient using the following formula (Eq. 5).

$$X_a = -1.15(X_a NDVI - 0.61) \tag{5}$$

The soil protection coefficient (X_a) takes values ranging from 0.01, in the case of strong protection by vegetation cover, to 1 when this protection is absent.

Soil erodibility coefficient (*Y*). The soil erodibility coefficient (*Y*), a significant parameter in the EPM model, reflects the intrinsic vulnerability of the soil to erosive processes. To calculate it, we used Wischmeier and Smith's formula (Wisch-

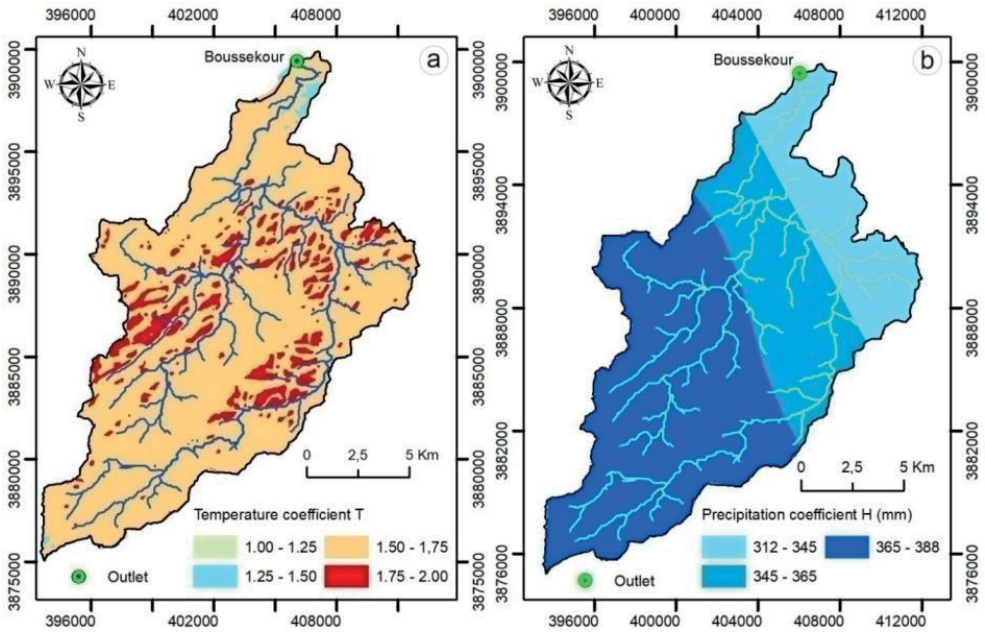

Fig. 3. Map of the Boussekour watershed: a) temperature coefficient *T*, b) precipitation coefficient *H*; source: own elaboration

meier and Smith, 1978), which incorporates the soil texture, its structure, its permeability, and its organic matter content (Eq. 6):

$$Y = \frac{2.1 \cdot M^{1.14} \cdot 10^{-4} \cdot (12 - OM) + 3.25 \cdot (\mathrm{S} - 2) + 2.5 \cdot (\mathrm{P} - 3)}{100} \quad (6)$$

where: Y = soil erodibility coefficient (–), OM = organic matter content (%), M = texture factor ((% silt + % fine sand) · (100 – % clay)) (–), S = structure code (–), P = permeability class (–).

The calculation of the soil erodibility coefficient (Y) required soil data from laboratory analyses of soil samples taken from points selected based on soil typology and the surface cover (Fig. 4) using a corer with a diameter of 7.5 cm and a length of 40 cm (Photo 1).

The particle size distribution of these samples (clay, silt, and fine sand) was determined by wet sieve analysis, while the organic matter content was measured by the loss on ignition method. Structure and permeability codes were assigned based on the texture classes identified, following the methodological recommendations of Denholm, Irvine and Schut (1993). The spatial distribution map of the soil erodibility coefficient (Y) was then generated by interpolating the Y-values of each soil sample (Tab. 1) using IDW interpolation in ArcGIS Pro.

Current erosion coefficient (φ). The φ coefficient reflects the intensity of erosive processes within the watershed, with values ranging from 0.1 (indicating slightly eroded areas) to 1 (indicating severely degraded zones), according to the classification proposed by Gavrilović (1988). In the Boussekour watershed, φ was estimated based on soil reflectance, which is assumed to correlate with the degree of degradation, following the methodology developed by Zorn and Komac (2009), and adapted by Chaaouan *et al.* (2013) according to Equation (7):

$$\varphi = \sqrt{\frac{OLI4}{Q_{\max}}} \quad (7)$$

where: $OLI4$ = band 4 Landsat 8/9; $Q_{\max}$ = radiance maximum of band 4 ($Q_{\max}$ = 65,535).

However, in areas with red soils, high natural reflectance may lead to overestimations; therefore, the use of the brightness index is recommended for a more accurate assessment (Lakhili *et al.*, 2021).

Slope coefficient (J_a). The slope contributes significantly to water erosion intensity, as confirmed by several previous studies (Wischmeier and Smith, 1978; Nearing, 1997; Morgan, 2009). An increase in slope gradient promotes faster surface runoff, which itself becomes a major erosive agent, often surpassing the energy exerted by raindrop impact (Wischmeier and Smith, 1978).

The slope coefficient (J_a) was derived from the 30 m resolution digital elevation model (DEM) using ArcGIS's Slope tool, with homogeneous polygons subsequently classified into five slope classes.

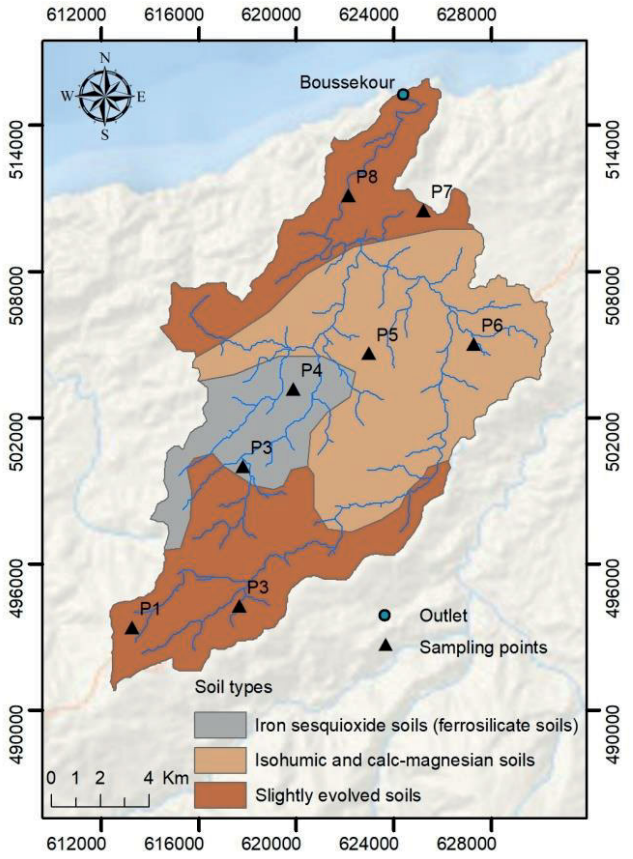

Fig. 4. Sampling points location in the Boussekour watershed; source: own elaboration

Photo 1. Soil sampling (a), and iron sesquioxide soil (b) in the Boussekour watershed (phot.: *A. Tawfik*)

Table 1. Erodibility coefficient of the soil samples analysed and their pedological characteristics

Soil sample	*OM* (%)		Sand (%)		Silt (%)		Clay (%)		S	P	*Y*	
	mean	*SD*	mean	*SD*	mean	*SD*	mean	*SD*			mean	*SD*
P1	3.52	0.02	29.04	0.37	33.93	0.41	3.17	0.05	3.00	3.00	0.40	0.003
P2	2.58	0.05	31.10	0.13	20.41	0.33	2.50	0.07	3.00	3.00	0.36	0.002
P3	2.82	0.02	19.26	0.32	54.74	0.21	2.91	0.08	4.00	4.00	0.57	0.002
P4	2.12	0.01	35.23	0.16	43.32	0.33	2.76	0.07	3.00	3.00	0.58	0.003
P5	3.08	0.02	35.81	0.41	44.06	0.16	1.67	0.04	3.00	3.00	0.54	0.003
P6	2.89	0.01	39.38	0.44	44.80	0.38	3.53	0.08	3.00	3.00	0.57	0.004
P7	2.32	0.01	21.79	0.30	27.64	0.16	3.40	0.02	3.00	3.00	0.35	0.002
P8	2.31	0.03	27.88	0.45	39.54	0.26	3.98	0.04	3.00	3.00	0.48	0.004

Explanations: *OM* = organic matter, S = structure code, P = permeability class, *Y*= soil erodibility coefficient, *SD* = standard deviation.
Source: own study.

RESULTS AND DISCUSSION

RESULTS

Soil protection coefficient (X_a)

The results obtained in the Boussekour watershed (Fig. 5a) reveal that 61.23% of its area is weakly protected ($0.41 \leq X_a \leq 0.60$), primarily consisting of agricultural land, seasonal crops, and degraded areas. This is followed by the medium protection class ($0.21 \leq X_a \leq 0.40$), which corresponds to open scrubland or partially covered paths, occupying around 37.77% of the territory. By contrast, areas benefiting from high protection ($X_a < 0.20$), thanks to dense vegetation formations, remain very scarce and cover only 0.69% of the total catchment area.

Soil erodibility coefficient (*Y*)

The results obtained (Fig. 5b) indicate that the soil erodibility coefficient (*Y*) in the Boussekour watershed varies from 0.35 to 0.58. This range includes a dominant class between 0.35 and 0.50, which represents a medium resistance to erosion and occupies 54.37% of the area, and a second class between 0.50 and 0.58, which reflects a low resistance to erosion and covers 45.61% of the area.

Current erosion coefficient (φ)

The results obtained by applying this equation show that the highest values were observed mainly in the central part ($\varphi = 0.74$), whereas the lowest values ($\varphi = 0.38$) were found in the northern and southern ends of the Boussekour watershed (Fig. 5c).

Slope coefficient (J_a)

Steep slopes (>20%) dominate the Boussekour watershed (Fig. 5c), covering 44.29% of its area, while gentle slopes (<10%) represent only 22.68%. Moderately sloped terrain accounts for the remaining 33.03%.

Erosion intensity coefficient (*Z*)

The erosion intensity coefficient (*Z*) is a dimensionless parameter developed to assess the overall intensity of erosive processes in each catchment. This coefficient integrates the combined influence of soil protection, soil erodibility, topography, and the current erosion indicator.

The results obtained (Tab. 2) show that the majority of the Boussekour watershed (45.97%) consists of areas where the *Z* coefficient exceeds 1, thus reflecting very high erosion intensity. This category is followed by the high-intensity class (0.7–1.0), which accounts for 30.93% of the basin. Moderate erosion ranks third, covering 20.18% of the area. Conversely, zones with low and very low intensity erosion together account for only 2.89% of the surface area.

Estimation of annual soil loss volume (*W*)

The application of the EPM model developed by Gavrilović to the Boussekour watershed enabled the production of a detailed map of specific soil losses resulting from water erosion by integrating all the factors influencing this process. The volumes of soil loss were initially estimated in $m^3 \cdot km^{-2} \cdot yr^{-1}$ (Fig. 6a). To facilitate agronomic and environmental interpretation, these values were then converted into $Mg \cdot ha^{-1} \cdot yr^{-1}$ (Fig. 6b) using Equation (8):

$$W\left(\mathrm{Mg} \cdot \mathrm{ha}^{-1} \cdot \mathrm{yr}^{-1}\right) = W\left(\mathrm{m}^3 \cdot \mathrm{km}^{-2} \cdot \mathrm{yr}^{-1}\right) \cdot sd\left(\mathrm{Mg} \cdot \mathrm{m}^{-3}\right) \cdot 10^{-2} \quad (8)$$

where: *sd* = soil density.

Finally, the quantification of annual soil loss (*W*) in the Boussekour catchment using the EPM method reveals that the high (20–40 $Mg \cdot ha^{-1} \cdot yr^{-1}$) and very high (40–80 $Mg \cdot ha^{-1} \cdot yr^{-1}$) erosion classes predominate, affecting together 62.63% of the total area (Fig. 7). In contrast, the lowest classes account for less than 9%. Thus, the average annual soil loss was estimated at 21.28 $Mg \cdot ha^{-1} \cdot yr^{-1}$.

DISCUSSION

The results of the assessment of erosion intensity within the Boussekour catchment by applying the Gavrilović EPM method reveal a major issue. Indeed, more than 76.9% of its area shows an erosion intensity classified as high to very high ($Z > 0.7$), amounting to an estimated mean annual loss of 21.28 $Mg \cdot ha^{-1} \cdot yr^{-1}$, which far exceeds the acceptable thresholds in the Mediterranean region.

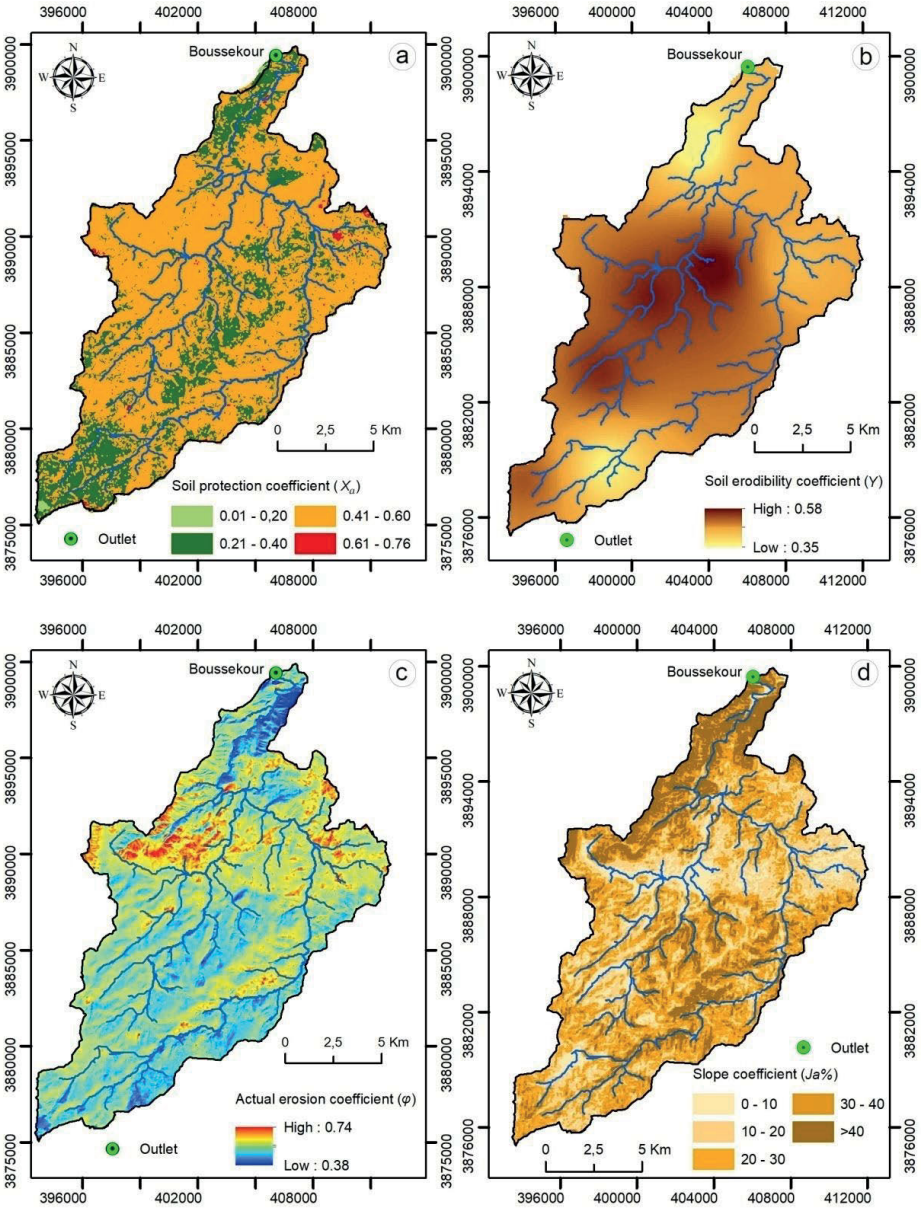

Fig. 5. Map of erosion characteristics in the Boussekour watershed: a) soil protection coefficient X_a, b) soil erodibility coefficient Y, c) current erosion coefficient φ, d) slope coefficient J_a; source: own study

Table 2. Erosion intensity coefficient (Z) values

Erosion intensity level	Classes of Z coefficient	Surface area	
		ha	%
Very low	<0.2	34	0.16
Low	$0.2 \leq Z < 0.4$	563	2.73
Moderate	$0.4 \leq Z < 0.7$	4,153	20.18
High	$0.7 \leq Z < 1$	6,366	30.93
Very high	>1.0	9,460	45.97

Source: own study.

There are many factors involved in this intense erosive dynamic:

- the topography of the basin, characterised by remarkably steep terrains (over 40% of the surface presents slopes >12%), thus favouring runoff and, consequently, the triggering of severe erosive processes;
- the friability of the substrates, linked to the predominance of flysch and marly-limestone formations of the Central Rif, particularly sensitive to detachment by runoff, which constitutes a major aggravating factor;
- the reduction of the vegetation covers, following deforestation, overgrazing, fires and slope cultivation, which offers poor soil protection;
- finally, anthropogenic factors, such as cereal cultivation on steeply sloping land without anti-erosion measures, playing an accelerating role in erosion.

These results are close to those observed in other watersheds of Moroccan mountainous regions, such as the Rif and the Atlas. As an illustration, in the Central Rif, Ed-Dakiri *et al.* (2024) quantified a mean soil loss of 24 $Mg \cdot ha^{-1} \cdot yr^{-1}$ in the Nekkor watershed using the RUSLE method, while Taher *et al.* (2022) measured 19 $Mg \cdot ha^{-1} \cdot yr^{-1}$ in the Ghiss basin using the USLE

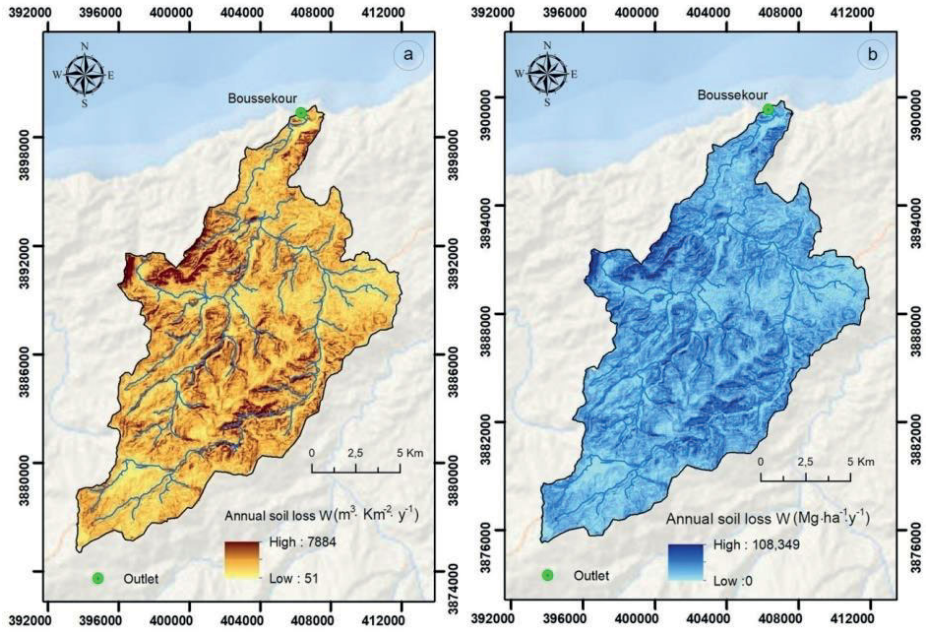

Fig. 6. Map of annual soil losses in the Boussekour watershed: a) in $m^3 \cdot km^{-2} \cdot yr^{-1}$, b) in $Mg \cdot km^{-2} \cdot yr^{-1}$; source: own study

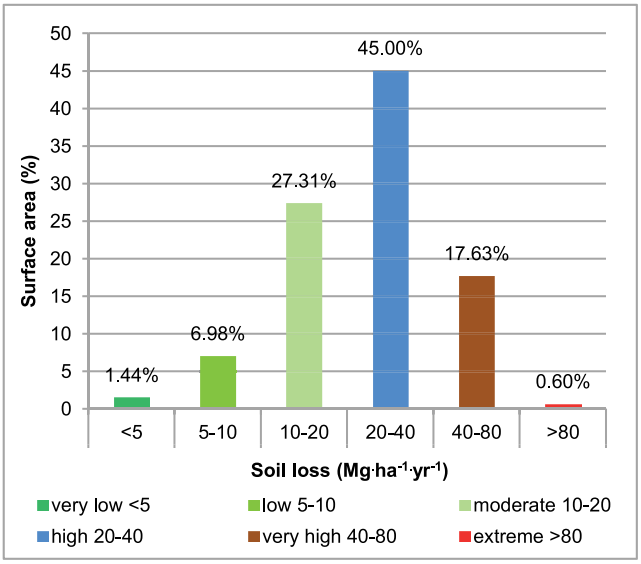

Fig. 7. Histogram of soil loss percentages by surface class in the Boussekour watershed; source: own study

method – values close to the Boussekour rate. Similarly, Tahouri *et al.* (2022) reported an average loss of 17.5 $Mg \cdot ha^{-1} \cdot yr^{-1}$ in the Oued Asfalou (North-eastern Rif). In contrast, Bachaoui *et al.* (2014) reported extreme losses of 35 $Mg \cdot ha^{-1} \cdot yr^{-1}$ in the Eastern High Atlas, with a marked concentration in the most degraded areas.

In summary, the results obtained for the Boussekour watershed, which exceed the tolerance threshold ranging from 1 to 12 $Mg \cdot ha^{-1} \cdot yr^{-1}$ (Roose, 1996), confirm a regional trend in the Mediterranean and semi-arid region (Mnasri *et al.*, 2025) where soil water erosion constitutes an increasing threat to the sustainability of agro-sylvo-pastoral ecosystems. In Morocco, for example, soil productivity losses, where water erosion is strongly implicated, are estimated at 2.1 bln US dollars per year (Laamouri and Khattabi, 2025), particularly in the northern catchment areas, with erosion rates reaching 14,700 $Mg \cdot yr^{-1}$ (Pérez-Cutillas *et al.*, 2025). This finding necessitates deploying targeted studies against erosion in these vulnerable areas, as well as anti-erosive strategies adapted to the socio-economic and institutional factors specific to each zone (Mnasri *et al.*, 2025).

CONCLUSIONS

This research sought to evaluate and map soil erosion vulnerability in the Boussekour catchment, whose downstream area is included within a protected area, through the application of the Gavrilović erosion potential method (EPM) approach. The use of GIS tools, data provided by remote sensing (RS), and those obtained through pedological soil analyses enabled us to carry out a sufficiently reliable analysis of erosion in our study area. The results obtained revealed that the majority of the land in the Boussekour catchment is affected by water erosion rates ranging from moderate to very high, and that the main annual soil loss for the entire area was 21.28 $Mg \cdot ha^{-1} \cdot yr^{-1}$.

Even though Gavrilović's EPM method is frequently adopted for the estimation of water erosion, it reveals certain weaknesses. Indeed, it is based on an empirical approach that does not model the actual dynamics of erosive processes. Moreover, the weightings assigned to certain classes depend heavily on the operator's judgement, which may affect the reliability of the results. The method remains static and sensitive to the quality of input data; it therefore requires validation and calibration, notably through magnetic susceptibility as a perspective, as well as a sound knowledge of the field to be applied in contexts different from the one for which it was originally designed.

This result underscores the necessity of implementing soil conservation practices to prevent the intensification of erosion processes, which now constitute a threat to the natural environment and cultivated lands of the region. These interven-

tions must prioritise sloping lands characterised by nearly non-existent vegetation cover and long exploited for cereal cultivation. These areas account for nearly two-thirds of the watershed, whereas the remaining third is less threatened by erosive phenomena. This section is located either at the northern and southern extremities, where vegetation cover remains significant, or on the relatively flat terrain situated in the central part of our study area.

ACKNOWLEDGEMENTS

We express sincere thanks to Mr Souahail Karim, Director of Al Hoceima National Park, for data access and Ms. Yasmin Messaaoudi and Mr. Younes Oubaki for their contributions in language editing and GIS support. We would also like to thank the reviewers whose recommendations contributed to improving this work. Their insights were invaluable in refining our analysis of soil erosion patterns.

CONFLICT OF INTERESTS

All authors declare that they have no conflict of interests.

REFERENCES

Akalai, N. *et al.* (2014) "Risk of water erosion in coastal watersheds north of Tetuan (Internal Rif, northern Morocco): Evidences from GIS-based spatial approach," *International Journal of Innovation and Applied Studies*, 8(4), 1735. Available at: https://ijias.issr-journals.org/abstract.php?article=IJIAS-14-245-13 (Accessed: January 01, 2023).

Bachaoui, M. *et al.* (2014) "Modeling and mapping water erosion risks in the High Atlas of Morocco: The Atlas of Beni Mellal as a case in point," *Journal of Remote Sensing and GIS*, 2(1), pp. 40–47. Available at: https://www.researchgate.net/publication/289538248_Modeling_And_Mapping_Water_Erosion_Risks_In_The_High_Atlas_Of_Morocco_The_Atlas_Of_Beni_Mellal_As_A_Case_In_Point (Accessed: January 01, 2023).

Borrelli, P. *et al.* (2017) "An assessment of the global impact of 21st century land use change on soil erosion," *Nature Communications*, 8(1), 2013. Available at: https://doi.org/10.1038/s41467-017-02142-7.

Bou Kheir, R., Girard, M.C. and Khawlie, M. (2001) "Erosion hydrique des sols dans les milieux méditerranéens: une revue bibliographique [Water erosion of soils in Mediterranean environments: A literature review]," *EGS – Étude et Gestion des Sols*, 8, pp. 231–245. Available at: https://www.scribd.com/document/666309411/erosion-hydrique (Accessed: February 03, 2023).

Chaaouan, J. *et al.* (2013) "Télédétection, SIG et modélisation de l'érosion hydrique dans le bassin versant de l'oued Amzaz, Rif Central [Remote sensing, GIS and modeling of water erosion in the Amzaz watershed, Central Rif]," *Revue française dephotogrammétrie et de télédétection*, 203, pp. 19–25. Available at: https://doi.org/10.52638/rfpt.2013.26.

Defour, T. (2015) *EIP-AGRI Focus group soil organic matter in Mediterranean regions. Final report*. Brussels: European Network for Rural Development. Available at: https://eu-cap-network.ec.europa.eu/publications/eip-agri-focus-group-soil-organic-matter-content-mediterranean-regions-final-report_en#section–resources (Accessed: September 28, 2023).

Denholm, K.A., Irvine, D.E. and Schut, L.W. (1993) *Field manual for describing soils in Ontario*. 4th edn. Guelph, Ontario: Ontario Centre for Soil Resource Evaluation. Available at: https://books.google.co.ma/books/about/Field_Manual_for_Describing_Soils_in_Ont.html?id=0zjAAQAACAAJ&redir_esc=y (Accessed: January 25, 2023).

Dragičević, N., Karleuša, B. and Ožanić, N. (2016) "A review of the Gavrilović method (erosion potential method) application," *Građevinar*, 68(9), pp. 715–725. Available at: https://doi.org/10.14256/JCE.1602.2016.

Ed-Dakiri, S. *et al.* (2024) "Assessing soil erosion risk through geospatial analysis and magnetic susceptibility: A study in the Oued Ghiss dam watershed, Central Rif, Morocco," *Scientific African*, 26, e02401. Available at: https://doi.org/10.1016/j.sciaf.2024.e02401.

Franchis de, L. (2003) *Threats to soils in Mediterranean countries. Document review*. Sophia Antipolis: Plan Bleu Centre d'activités régionales. Available at: https://planbleu.org/sites/default/files/publications/cahiers2_sols_us.pdf (Accessed: January 07, 2023).

Gavrilović, Z. (1988) "Use of an empirical method (erosion potential method) for calculating sediment production and transportation in unstudied or torrential streams," in W.R. White (ed.) *International Conference on River Regime*, Wallingford, UK, 18–20 May 1988. Chichester, New York: Published on behalf of Hydraulics Research Ltd., Wallingford: J. Wiley, p. 411–422.

HCEFLCD (1996) *Plan National d'Aménagement des Bassins Versants (PNABV) [National Watersheds Development Plan]*. Kénitra: *Haut Commissariat aux Eaux et Forêts et à la Lutte Contre la Désertification.*

HCEFLCD (2013) *Le Programme d'Action National de Lutte Contre la Désertification : Actualisation et adaptation aux spécificités zonales. Rapport principal [National Action Program to Combat Desertification: Update and adaptation to zonal specificities]*. Kénitra: Haut Commissariat aux Eaux et Forêts et à la Lutte Contre la Désertification. Available at: http://www.abhatoo.net.ma/maalama-textuelle/developpement-economique-et-social/developpement-economique/environnement/desertification/le-programme-d-action-national-de-lutte-contre-la-desertification-actualisation-et-adaptation-aux-specificites-zonales (Accessed: March 20, 2025).

Hudson, N.W. (1990) *Conservation des sols et des eaux dans les zones semi-arides [Soil and water conservation in semi-arid areas]*. Rome: FAO. Available at: https://horizon.documentation.ird.fr/exl-doc/pleins_textes/divers15-05/39357.pdf (Accessed: January 25, 2023).

Kosmas, C. *et al.* (1997) "The effect of land use on runoff and soil erosion rates under Mediterranean conditions," *Catena*, 29(1), pp. 45–59. Available at: https://doi.org/10.1016/S0341-8162(96)00062-8.

Laamouri, A. and Khattabi, A. (2025) "Estimating the economic cost of land degradation and desertification in Morocco," *Land*, 14(4), 837. Available at: https://doi.org/10.3390/land14040837.

Lakhili, F. *et al.* (2021) "GIS-based soil erosion estimation using EPM method in the Beht catchment," *Environmental and Water Sciences, public Health and Territorial Inteligence Journal*, 5(2), pp. 588–596.

Lal, R. (2001) "Soil degradation by erosion," *Land Degradation & Development*, 12, pp. 519–539. Available at: https://doi.org/10.1002/ldr.472.

Milevski, I. *et al.* (2024) "Multi-hazard modeling of erosion and landslide susceptibility at the national scale in the example of

North Macedonia," *Open Geosciences*, 16(1), 20220718. Available at: https://doi.org/10.1515/geo-2022-0718.

Ministère de la Transition Energétique et du Développement Durable (2020) *4ème Rapport sur l'état de l'environnement au Maroc. Version intégrale [4th Report on the State of the Environment in Morocco. Full version]*. Rabat: Ministère de la Transition Energétique et du Développement Durable. Available at: https://www.environnement.gov.ma/images/2021/rapport/REEM4-VERSION_INTEGRALE.pdf (Accessed: May 15, 2025).

Mnasri, H. *et al*. (2025) "Water soil erosion in the Mediterranean and semi-arid region: Bibliometric analysis (2002–2023)," *Euro-Mediterranean Journal for Environmental Integration*, 10, pp. 4565–4574. Available at: https://doi.org/10.1007/s41207-025-00864-5.

Morgan, R.P.C. (2009) *Soil erosion and conservation*. 3rd edn. Hoboken: John Wiley & Sons.

Nearing, M.A. (1997) "A single, continuous function for slope steepness influence on soil loss," *Soil Science Society of America Journal*, 61(3), pp. 917–919. Available at: https://doi.org/10.2136/sssaj1997.03615995006100030029x.

Pérez-Cutillas, P., Benabdelouahab, S. and Salhi, A. (2025) "Mitigating erosion and enhancing sediment retention: A modeling approach to sustainable land management," *Earth Systems and Environment*. Available at: https://doi.org/10.1007/s41748-025-00660-9.

Roose, E. (1996) "Land husbandry: components and strategy," *FAO Soils Bulletin*, 70. Rome: FAO. Available at: https://www.fao.org/4/t1765e/t1765e00.htm (Accessed: April 02, 2025).

Shakesby, R.A. (2011) "Post-wildfire soil erosion in the Mediterranean: Review and future research directions," *Earth-Science Reviews*, 105(3–4), pp. 71–100. Available at: https://doi.org/10.1016/j.earscirev.2011.01.001.

Taher, M. *et al*. (2022) "An estimation of soil erosion rate hot spots by integrated USLE and GIS methods: A case study of the Ghiss Dam and Basin in Northeastern Morocco," *Geomatics and Environmental Engineering*, 16, pp. 95–110. Available at: https://doi.org/10.7494/geom.2022.16.2.95.

Voltz, M. *et al*. (2018) "Mediterranean land systems under global change: Current state and future challenges," *Regional Environmental Change*, 18, pp. 619–622. Available at: https://doi.org/10.1007/s10113-018-1292-z.

Wischmeier, W.H. and Smith, D.D. (1978) "Predicting rainfall erosion losses: A guide to conservation planning," *Agriculture Handbook*, 537). Washington, D.C.: USDA. Available at: https://www.ars.usda.gov/ARSUserFiles/60600505/RUSLE/AH_537%20Predicting%20Rainfall%20Soil%20Losses.pdf (Accessed: May 05, 2025).

Zahnoun, A.A. *et al*. (2019) "Estimation and cartography the water erosion by integration of the Gavrilovic "EPM" model using a GIS in the Mediterranean watershed: Lower Oued Kert watershed (Eastern Rif, Morocco)," *International Journal of Advance Research, Ideas and Innovations in Technology*, 5(6), pp. 367–374. Available at: https://www.ijariit.com/manuscripts/v5i6/V5I6-1298.pdf (Accessed: June 26, 2025).

Zeghmar, A., Marouf, N. and Mokhtari, E. (2022) "Assessment of soil erosion using the GIS-based erosion potential method in the Kebir Rhumel Watershed, Northeast Algeria," *Journal of Water and Land Development*, 52, pp. 133–144. Available at: https://doi.org/10.24425/jwld.2022.140383.

Zorn, M. and Komac, B. (2009) "Response of soil erosion to land use change with particular reference to the last 200 years (Julian Alps, Western Slovenia)," *Revista de geomorfologie*, 11, pp. 39–47. Available at: https://www.geomorfologie.ro/wp-content/uploads/2015/07/Revista-de-geomorfologie-nr.-11-2009-05.zorn_.pdf (Accessed: June 10, 2025).